Grinding assistance in the transformation of gibbsite to corundum

Rosa M. Torres Sánchez[a)]
Centro de Tecnología en Recursos Minerales y Cerámica (CETMIC), Camino Centenario y 506, C.C. 49, 1897 Gonnet, Argentina

A. Boix
Instituto de Calalisis y Petroquimica -Universidad Nacional del Litoral, Santiago del Estero 2829, 3000 Santa Fe, Argentina

R.C. Mercader
Departamento de Física, IFLP, Facultad de Ciencias Exactas, Universidad Nacional de La Plata, Argentina

(Received 26 February 2001; accepted 14 January 2002)

After gibbsite was milled for 5 min in a Cr-steel oscillating mill, corundum was obtained by heating the powder for 3 h at 800 °C. We found that iron contamination, produced by the milling process, is essential to attain the transformation at this low temperature and is located at the surface of the gibbsite particles. The knowledge of the oxidation state and location of the contaminant elements, necessary to control the solid-state reactions and/or phase transformations induced by the milling, was realized in this work by a characterization performed by chemical analysis, x-ray photoelectron spectroscopy, Mössbauer spectroscopy, and isoelectric point determination. The iron contamination amounted to about 3% (as Fe_2O_3) for the sample milled for 60 min. That the iron contamination that occurred mainly on the gibbsite amorphous surface was concluded after a comparison of the isoelectric point determination of the milled samples with that of a mechanical mixture of gibbsite and hematite. X-ray diffraction studies showed that gibbsite looses its crystallinity after the first 5 min of milling.

I. INTRODUCTION

Milling techniques allow an intimate blend of materials and, promoting the interdiffusion of the initial components, facilitate their chemical reactions and crystalline phase transformations.[1] The dehydration of gibbsite, γ–$Al(OH)_3$, is a clear example of the influence of mechanical activation.[2]

Mechanically induced processes, such as impact, friction, or compression, are complex and sometimes render seemingly contradictory results.[3] For example, the dependence of the intensity and type of mechanical stress on the type of mill is found not to be directly connected to the products obtained.[3] However, it is known that the mechanochemical changes produced by milling occur mainly in regions close to the grains surface, where the material is mostly affected by abrasion and repeated collisions with other grains and with the milling tools.[4]

Corundum, α–Al_2O_3, is widely used in a variety of technological applications since it is one of the hardest known materials, can be prepared in some forms with a high surface area, and is chemically inert. However, it is relatively expensive mainly because of the cost of the raw chemicals and the relatively high temperatures (1200 °C) needed for its manufacture. For this reason, cheaper precursors (like gibbsite) and lower transformation temperatures have been explored as a means of cost reduction in the industrial applications of corundum. In particular, the transformation temperature required in the sequence of intermediate phases from gibbsite to corundum was found to be modified by the milling activation of gibbsite.[5]

The effect of impurities on the corundum formation at lower temperatures has been known for some time; e.g., a temperature decrease of 200 °C was observed when a mixture of 5% hematite and other metallic oxides was added to gibbsite powders.[6] Recently, a low-temperature route to obtain corundum has been reported,[7] but the high cost of the sol-gel raw materials minimizes its possible industrial usage.

In this work, toward attaining smaller particle sizes and hence to increase the surface area of the final material, we activated gibbsite by milling. We also found, as a byproduct of important economic consequence, that the

a)e-mail: rosats@netverk.com.ar

iron contamination from the steel mill allows significantly lower temperatures to obtaining corundum from gibbsite.

II. MATERIALS AND METHODS

Gibbsite powder of particle size 44–74 μm supplied by Duperial (Argentina). was used as the starting milling material. The chemicals used for comparison purposes were pure commercial hematite (α–Fe_2O_3; 99%), supplied by BDH (Belgium), and pure commercial corundum with particle size <0.5 μm, supplied by Alcoa (Brazil).

A Herzog HSM 100 (Germany) oscillating mill was loaded with a maximum amount of 40g gibbsite. The milling chamber consisted of a hollow Cr-steel cylinder, and the milling tools were a ring and a solid cylinder of the same material. The sample was distributed in the spaces between these pieces.

After the milling chamber was loaded, the total times were attained by milling during periods of 120 s with stops of 4 h to avoid heating the milling chamber and powder. These samples were named according to the total milling time in minutes, namely, 0, 5, 20, and 60 min. Afterwards, all samples were heated for 3 h at 500, 800, 900, and 1250 °C and noted correspondingly to the grinding time in minutes followed by the temperature of thermal treatment, e.g., 0-500, 20-800, 60-500, etc.

X-ray diffraction (XRD) patterns were obtained in a Philips PW 1140 diffractometer using Cu K_α radiation and a Ni filter. The working conditions were 40 kV and 20 mA. Samples were analyzed by means of the powder mounting technique. The amount of corundum in each sample was determined by comparing the diffracted intensity area of the peak at 43.27° (2θ) (2.09Å, *hkl* = 113) with that of a pure corundum commercial sample considered as 100%.

X-ray photoelectron spectroscopy (XPS) analyses were performed in an ESCA Shimadzu 750 spectrometer with an Escapac 750 system. A Mg anode (1253 eV) operating at 30 mA and 8 mV was used as the excitation source in a residual vacuum of 10^{-5} Pa. An energy correction was made to account for the sample charging based on the C 1*s* peak at 285 eV. The integrated area of the peaks and their measured full width at half-maximum (FWHM) were normalized. Isoelectric point (IEP) determinations were performed by means of the measurement of the diffusion potential, from which the transport number (t^+) value was obtained in the same way as described before.[8–10] The IEP is defined as the value of the pH when the surface is not charged. Its value is obtained from the t^+–pH curve; it is the pH when both cations and anions in the sample have equal mobility, and this happened at $t^+ = 0.5$. Because the t^+ values belong to all cations (adsorbed and free) contained in the sample, when the amount of free ions is 100 times less than that of the adsorbed ones,[11] the calculated t^+ value is considered to correspond to the adsorbed ion (counter ion) and then the IEP can be determined. Mössbauer spectra were taken at room temperature in transmission geometry in a conventional constant acceleration spectrometer of 512 channels with a 50mCi nominal activity $^{57}Co\langle U\rangle Rh\langle U\rangle$ source. The spectra were fitted with a nonlinear least-squares program with constraints assuming Lorentzian line-shapes. Isomer shifts (δ) were referred to α–Fe at room temperature. Differential thermal analyses (DTA) were obtained in a Netzsch simultaneous thermal analyzer STA 409, in nitrogen atmosphere and with a heating rate of 10 K/min. The specific surface areas of the samples at different grinding times were determined by N_2 adsorption [Brunauer–Emmett–Teller (BET) method]. The percentage of iron oxide in sample 60 was determined by previous oxidation and $K_2Cr_2O_7$ titration.

III. RESULTS AND DISCUSSION

Figure 1 shows the XRD patterns of the samples for different milling times. The line broadening, which increases with milling time, is coincident with previous observations[2,5] and indicates a progressive loss of crystalline order.

From the two XPS spectral signals recorded (Al 2*p* and O 1*s*), we calculated the binding energies (E_b) and FWHM values shown in Table I. The relative spectral areas O 1*s*/Al 2*p*, Fe 2*p*/Al 2*p,* and C 1*s*/Al 2*p,* as well as the BET specific surfaces are also displayed. These ratios indicate that iron and carbon contaminations (coming from the mill and the vacuum pump oil, respectively) alter the fraction of Al atoms at the surface.

The constant Al 2*p* and O 1*s* E_b and FWHM values indicate that the coordination of Al or O atoms at the surface is not modified by milling.[12] The decrease of the O/Al relationship with milling time follows the same trend as the C/Al ratio, indicating that the Al signal is screened by the carbon contamination. No Fe 2*p* signal was found in the initial sample and the one milled for 5 min. The small Fe/Al ratio found for the longer milling times suggests an increasing iron contamination of the alumina surface that can only originate in the milling tools. The iron amount determined in sample 60, by chemical analysis, indicates a surface contamination of about 3%, expressed as hematite.

The increase of specific surface with grinding time agrees with that obtained elsewhere for a different gibbsite sample.[2]

Figure 2 shows the Mössbauer spectrum for sample 60. Absorption profiles belonging to different iron species can be observed. One sextet, two doublets, and one singlet had to be used to obtain a good fitting of

the data. The central narrow peak at 0.0 mm/s (with respect to α–Fe) can be assigned[13] to very small superparamagnetic Fe^0 particles and amounts to 20 ± 3% of the total spectral area.

The doublets belonging to Fe^{2+} (with quadrupole splitting, $\Delta = 1.32 \pm 0.24$ mm/s, isomer shift with respect to α–Fe, $\delta = 1.40 \pm 0.12$ mm/s) and to Fe^{3+} ($\Delta = 0.63 \pm 0.05$ mm/s, $\delta = 0.28 \pm 0.06$ mm/s) contributed with relative areas of 13 ± 3% and 37 ± 9%, respectively. The sextet with broad lines (of hyperfine parameters with values of $H = 32.5 \pm 0.1$T, $\delta = 0.02 \pm 0.02$ mm/s, and $2\epsilon = -0.02 \pm 0.02$ mm/s, for the magnetic hyperfine field, isomer shift, and quadrupole shift, respectively) has a relative area of 30 ± 5% of the total spectrum. These values correspond to magnetically split Fe^0 atoms whose hyperfine fields are diminished by the small size of their particles—however larger than those involved in the Fe^0 superparamagnetic fraction—and also modified by the likely location of a considerable amount of atoms close to the gibbsite grains and in disordered regions of the sample.

Except for the Fe^{2+} doublet, where it is known that the recoil-less factor is about 20% lower than the f-factors of the other iron species,[14] the relative areas of the Mössbauer signals can be considered to correspond to the actual amount of atoms in the different oxidation states within the experimental errors. Under these assumptions, the total weight percent obtained for the detected iron oxidation states were 42%, 13%, and 31% for Fe^0, Fe^{2+}, and Fe^{3+}, respectively.

Figure 3 shows the t^+ curves against pH for all the samples. The value of IEP can be seen to increase from pH = 9.2 for sample 0 to pH = 12.5 for sample 5. At present, we do not have an explanation for this high IEP_{pH} value. An IEP_{pH} higher than 10 has never been reported for aluminum oxides or hydroxides. No iron contamination was detected by XPS for sample 5.

Milling times longer than 5 min caused an IEP_{pH} decrease from 12.5 to around 10.5 for samples 20 and 60, respectively. This could be attributed to the lower rate of decrease of the gibbsite particle as the milling progresses (particle size average diameters decreased from 50 to 20 μm after milling for 0 and 5 min, respectively, and remained constant for longer grinding times[2]).

If the gibbsite milled sample was only a mixture of gibbsite and hematite coming from the milling tools, and the iron contamination was not coating the gibbsite particles—as suggested by the XPS results—the IEP determination by diffusion potential of a specially prepared mixture (not milled) of hematite and pure gibbsite should yield the same value as the milled sample. That is, the IEP_{pH} of a mixture of phases and that of iron-coated

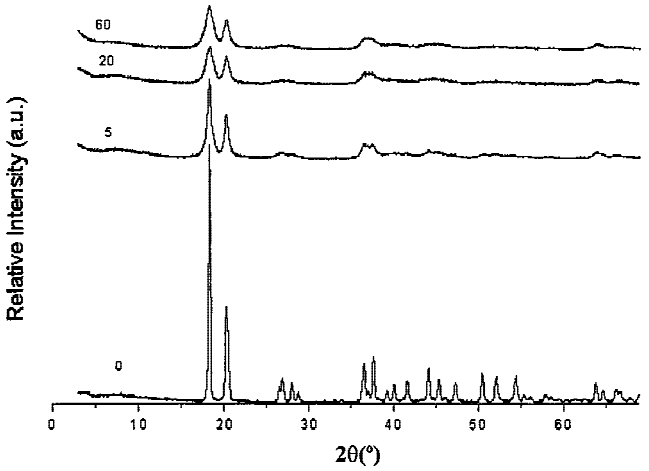

FIG. 1. X-ray patterns of gibbsite samples milled for the times shown.

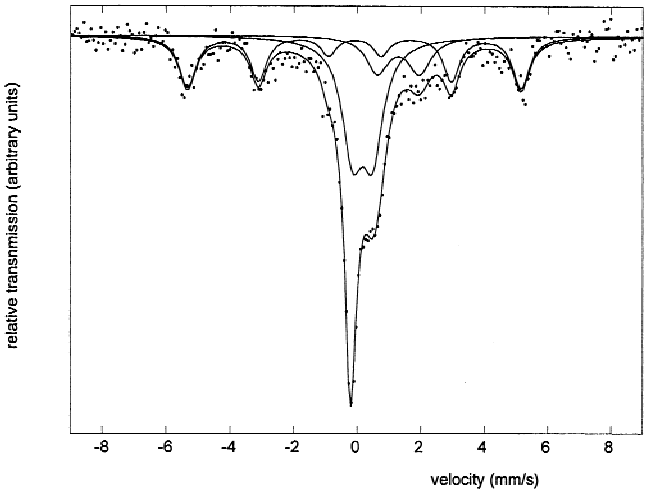

FIG. 2. Mössbauer spectrum of sample 60. The outer solid line is the least squares fitting of the data. The inner thin solid lines are the subspectra of the different iron species described in the text.

TABLE I. Binding energy values and FWHM for Al 2*p* and O 1*s* peaks and relationships between elements O 1*s*/Al 2*p,* Fe 2*p*/Al 2*p,* and C 1*s*/Al 2*p,* obtained by XPS and specific surface for the indicated samples. (n.d. = not detected).

Sample	Al 2*p* (eV) E_b (FWHM)	O 1*s* (eV) E_b (FWHM)	O 1*s*/Al 2*p* area ratio (%)	Fe 2*p*/Al 2*p* area ratio (%)	C 1*s*/Al 2*p* area ratio (%)	S (BET) (m^2/g)
0	74.3 (2.0)	532.2 (2.6)	2.20	n.d.	1.82	6
5	74.2 (2.0)	532.2 (2.7)	2.00	n.d.	1.74	25
20	74.3 (2.0)	532.3 (2.5)	1.98	0.03	1.60	41
60	74.2 (2.0)	532.2 (2.5)	1.80	0.03	1.45	107

gibbsite particles should not be the same. Figure 4 shows the t^+ against the pH curve for the mixture sample prepared with the same amounts of gibbsite and hematite as those found in sample 60. The IEP_{pH} values are not only different (10.0 for the mixture, and 10.5 for sample 60), but the t^+ dependence on pH is also totally different. These results suggest that there are different iron oxide–gibbsite associations in both samples. If this holds, it should be in agreement with the increase in the Fe/Al ratio measured by XPS, which is indeed confirmed by the values shown in Table I.

If we assume that only iron oxide (as hematite) coats the amorphized gibbsite particles, the apparent surface coverage (%ASC) can be calculated using the equation of Castillo *et al.*[15]

$$\%\mathrm{ASC} = \frac{M_{Fe}(IEP_G - IEP_{Fe/G})}{M_G(IEP_{Fe/G} - IEP_{Fe}) - M_{Fe}\,(IEP_{Fe/G} - IEP_G)} \quad ,$$

where M_{Fe} and M_G are the molecular weights of iron oxide and gibbsite, respectively, and the subscripts G, Fe/G, and Fe refer to the gibbsite, hematite–gibbsite, and hematite samples, respectively. The IEP data of the different samples are displayed in Fig. 3. The reported IEP_{pH} value of hematite is 8.0.[16] The %ASC values obtained for 20 and 60 samples were 5.3 and 9.8, respectively, which indicate the increasing iron coverage of gibbsite with milling time.

Figures 5 and 6 show the x-ray patterns of the samples with different heat treatments after the milling times specified. Independently of the milling time, the observation of Fig. 5 allows to infer that a temperature treatment at 500 °C forces all samples into a state very close to that of an amorphous one. The presence of γ– and κ–Al_2O_3 was revealed by the peaks at 1.38, 1.97, and 2.35 Å belonging to the (300), (202), and (110) reflections of γ–Al_2O_3, and those at 1.38, 1.60, and 2.08 Å to the (300), (116), and (113) ones of κ–Al_2O_3.

Figure 6 displays the diffraction patterns of the samples thermally treated at 800 °C. The beginning of the gibbsite-to-corundum transformation can already be observed in the pattern of sample 5-800. Samples 20-800 and 60-800 exhibit clear corundum peaks.

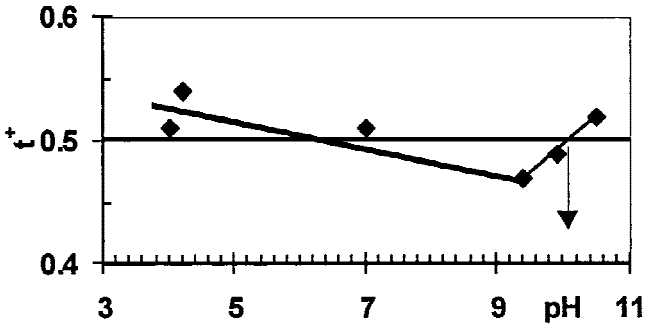

FIG. 4. Curve of t^+ versus pH for a mixture of gibbsite and hematite (relationship 10/0.1 wt%) purposely prepared for comparison. Solid lines are a guide for the eye.

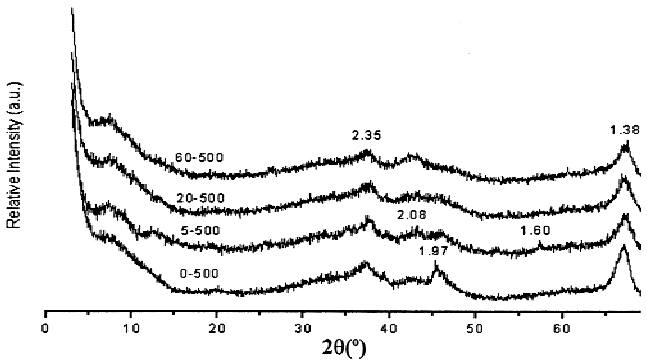

FIG. 5. X-ray patterns of samples milled for 0, 5, 20, and 60 min and further heat-treated at 500 °C for 3 h.The numbers on top of the data show the positions in Å belonging to the following Miller indices of the peaks: 0-500 sample 1.97(202) of γ–Al_2O_3; 5-500, 1.60(116) and 2.08 (113) of κ–Al_2O_3; 60-500 sample 1.38(300) and 2.35(110) of γ–Al_2O_3.

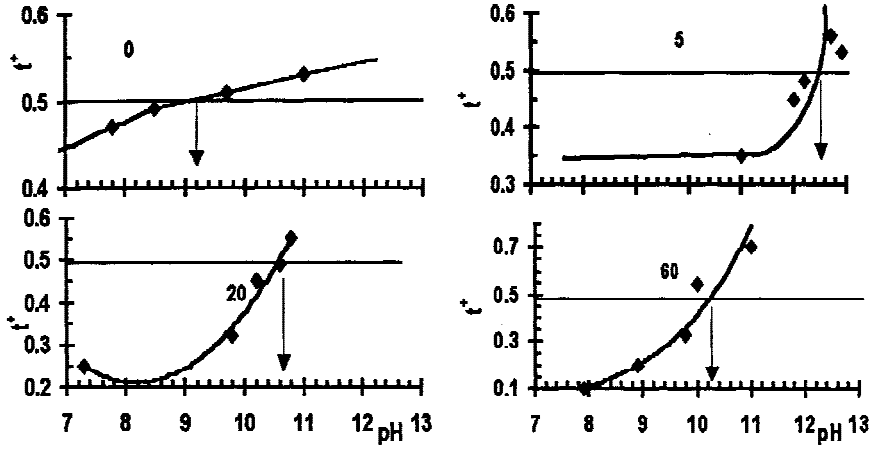

FIG. 3. Curves of t^+ against pH for samples 0, 5, 20, and 60. Solid lines are spline regressions meant only as a guide for the eye.

A further increase of the thermal treatment temperature to 900 °C (XRD pattern not shown) produces a further step of the transformation towards corundum in the same samples. The quantitative corundum transformation was determined in milled samples treated at 800 and 900 °C and is shown in Table II.

The corundum percentage increased considerably when the temperature was raised 100 °C from 800 to 900 °C. Almost all gibbsite in samples 20 and 60 was transformed to corundum when thermally treated at 900 °C for 3 h. In contrast, sample 0 (non-activated gibbsite) did not show any measurable amount of corundum. Peaks displayed in XRD patterns after a thermal treatment at 1250 °C (XRD figure not shown) indicate the complete transformation to corundum in all samples, including sample 0.

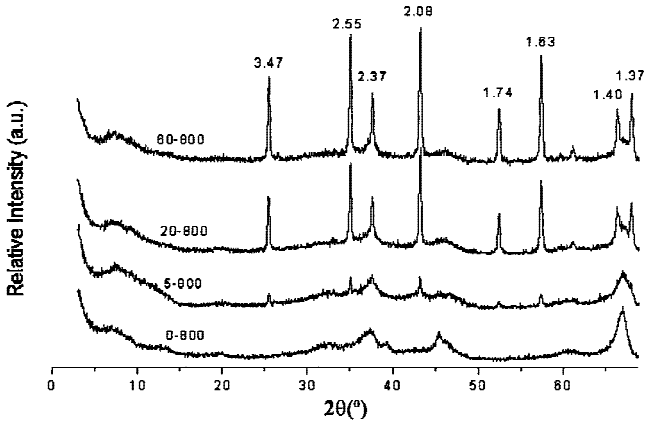

FIG. 6. X-ray patterns of samples milled for 0, 5, 20, and 60 min and further heat-treated at 800 °C for 3 h.The numbers on top of the 60-800 data show the positions in Å of peaks with the following Miller indices of corundum (α–Al_2O_3): 1.37(300), 1.40(214), 1.63(116), 1.79(024), 2.08(113), 2.37(110), 2.55(104), and 3.47(012).

TABLE II. Percentage of corundum obtained for all samples for thermal treatments at the indicated temperatures. (n.d. = not detected).

	Corundum (%)	
Sample	800 °C	900 °C
0	n.d.	n.d.
5	8	52
20	26	95
60	40	100

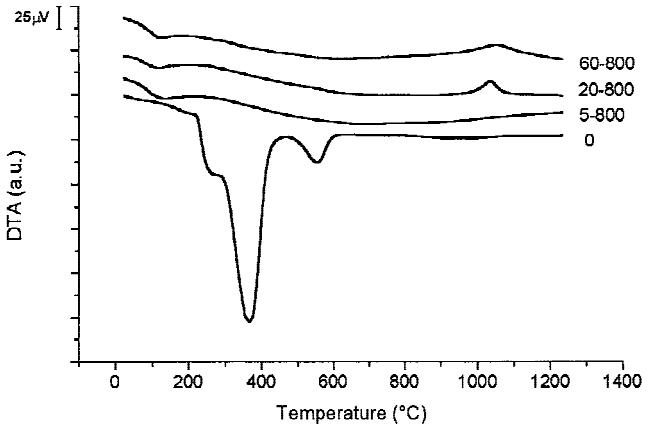

FIG. 7. DTA analyses of samples milled for 0, 5, 20, and 60 min and further heat-treated at 800 °C for 3 h.

Figure 7 shows the DTA analysis of the samples indicated. For sample 0, a large endothermic peak was observed at about 350 °C as well as a small one at about 500 °C. These peaks denote the formation of γ–AlOOH and its dehydroxylation, respectively.[17] The DTA analyses of 20-800 and 60-800 samples showed an exothermic peak at 1040 °C. This peak belongs to the transition to corundum and is in agreement with the 20-800 and 60-800 XRD patterns. However, the DTA of the 0-800 sample did not show any peak around these temperatures, also in agreement with the absence of any corundum peak in its XRD pattern.

IV. CONCLUSIONS

The activation of inexpensive gibbsite powders in an oscillating steel mill for about 20 min not only produces the usually observed increase of the surface area of the milled powder, but also allows corundum to be obtained from the final material by heating the powder for 3 h at 800 °C. This temperature is much lower than the 1200 °C typically required to induce the transformation. The iron contamination originated in the milling tools is essential for this reaction to occur.

The iron contamination, which amounts to about 3% (as hematite) after 60 min of milling, was observed to lie almost entirely at the surface of the gibbsite particles by several surface analytical techniques, in particular, by IEP.

ACKNOWLEDGMENTS

The authors gratefully acknowledge the technical assistance of J. Rinaldi and Lic. S. Conconi. Partial financial support by CONICET (PIPs 0217/98 and 4326) is thankfully acknowledged. R.M.T.S. and R.C.M. are members of Carrera del Investigador Científico-Scientist Research Center, CONICET, Argentina.

REFERENCES

1. O. Abe, Kona **13,** 159 (1995).
2. A. Scian, E.F. Aglietti, J.M. Porto Lopez, and E. Pereira, Lat. Am. J. Chem. Eng. Appl. Chem. **14,** 51 (1984)
3. T. Tsuchida and N. Ichikawa, React. of Solids. **7,** 207 (1989).
4. K.S. Venkataraman and K.S. Narayanan, Powder Technol. **3,** 190 (1998).
5. P. Clark and J. White, Trans. Brit. Ceram. Soc. **49,** 305 (1950).
6. Y. Wakao and T. Hibino, Nagoya Kogyo Gijutsu Shikensho Hokoku **11,** 588 (1962).

7. N. Bahlawane and T. Watanabe. J. Am. Ceram. Soc. **83,** 2324 (2000).
8. R.M. Torres Sánchez, H.J. Gasalla, and E. Pereira, React. Solids **7,** 53 (1989).
9. R.M. Torres Sánchez., J. Mater. Sci. Lett. **15,** 461 (1996)
10. M. Tschapek, R.M. Torres Sánchez, and C. Wasowski, Z. Pfl. Bodenk. **152,** 73 (1989).
11. M. Tschapek and I. Natale, Kolloid S. für Polymers **251,** 490 (1973).
12. R.M. Torres Sanchez, E. Basaldella, and J. F. Marco. J. Colloid Interf. Sci. **215,** 339 (1999).
13. F. Bødker, S. Mørup, C.A. Oxborrow, S. Linderoth, M.B. Madsen, and J.W. Niemantsverdriet, J. Phys. Condens. Matter **4,** 6555 (1992).
14. E. De Grave, S.G. Eeckhout, and C.A. McCammon, Hyperfine Interact. **122**, 21 (1999).
15. R. Castillo, B. Koch, P. Ruiz, and B. Delmon, in *Preparation of TiO_2 Supported on SiO_2 Catalysts: Study of the Dispersion and the Texture of TiO_2* (VI Internat. Symp. Sci. Bases Preparation Heterog. Catalysts, L-l-N. Belgium, 1994), p. 299.
16. G.A. Parks, Chem. Rev. **65**, 177 (1965).
17. R.C. Mackenzie, in *Differential Thermal Analysis,* edited by R.C. Mackenzie (Academic Press, London and NJ, 1970), p. 283.